REAL TIME PREDICTION OF COHERENT GENERATOR GROUPS

Emmanuel A. Frimpong[1], Johnson Asumadu[2] and Philip Y. Okyere[3]
[1,3]Kwame Nkrumah University of Science and Technology, Kumasi, Ghana
[2]Western Michigan University, Kalamazoo, Michigan, USA
[1]eafrimpong.soe@knust.edu.gh, [2]johnson.asumadu@wmich.edu, [3]pyokyere.soe@knust.edu.gh

Abstract: This paper presents a scheme for predicting coherent generator groupings that may result following a disturbance that leads to transient instability. The proposed scheme uses rotor speed deviations of the individual generators in the power system as input data, and a multilayer perceptron neural network as decision making tool. The speed deviations are extracted 5 cycles after the tripping of a line or bus following a disturbance. The proposed scheme is able to predict coherent generator groups before they are formed. The prediction accuracy of the scheme for 114 fault cases was found to be 91.22%

Key words: Generator coherency, Islanding, multi-layer neural networks, power system stability

1. Introduction

Most power systems are being operated with reduced stability margins. This is due to the huge demand for electric power which is fuelled by industrialization, modernization, and population growth. Limited installed generation capacity and unavailability or high cost of mechanical energy sources to drive the prime movers of generators have also contributed to the problem of operating power systems close to their stability limits.

The stability of such systems is endangered when subjected to large disturbances such as the tripping of transmission lines due to faults. Instability may lead to cascading system failures, which could cause equipment damage, pose safety hazards to personnel, contribute to cascading outages, and shutdown of large areas of or entire power systems [1, 2].

Whenever transient stability analysis of a system indicates that the system is approaching a catastrophic failure, control actions need to be taken in order to limit the extent of damage of the failure. One of such control actions is to separate the system into smaller islands at slightly reduced capacity. System islanding is often considered as one of the final stage of power system defense plans. The goal is to preserve stable areas of the faulted power system. Islanding also plays an important role in the power system restoration phase as it can make the power system restoration less complex and reduce the overall restoration time. The basis for islanding is not standard but rather depends on the nature of the utility. Even though the formation of islands is dominated by geographical proximity of the synchronous generators to maintain generation-load balance, there are some factors which can assist in designing a better islanding scheme. These factors include the type and location of the fault, and the dynamic performance of every island in the system against the fault [3, 4].

Research has gone into the development of controlled islanding schemes [3 – 8]. One of the important issues for controlled islanding is the determination of the separation interfaces to form islands. Coherent generator groups, load/generation balance, and other security criteria such as avoiding overloading of any transmission line within islands, need to be considered in order to determine separation interfaces. In addition, consideration should be given to whether the separation interfaces are topologically fixed or adaptive to changes of power-flow profiles or coherent generator groups. Due to topological characteristics of power systems, generators tend to form coherent groups oscillating with each other under disturbances. Coherent generation groups can be studied offline using, for example, slow coherency analysis technology. However, the actual out-of-step mode may not be angular separation between all those offline identified groups. Perhaps only one or two generators or generator groups go out of step from the other generators in the system. Therefore, the separation interfaces should be able to only separate actual out-of-step groups [9].

For effective damping control for online operation of power systems, it is essential to have an online adaptive coherency grouping approach [10, 11]. Such a scheme will set the boundaries of islands based on the nature of the disturbance. In pursuance of this, a number of methods for detecting coherent generators online to facilitate system separation have been proposed [10 – 19].

This paper makes a contribution to this ongoing research in adaptive coherency identification. It proposes a novel online scheme for predicting coherent generator groups that may be formed after a disturbance to improve the success rate of controlled islanding. The proposed scheme predicts coherent groups before they are formed. The scheme uses as inputs, the rotor speed deviations of the individual generators within the system. Trained multilayer perceptron neural networks (MLPNNs) are used to predict the coherent generator groups that are likely to be formed. The scheme was tested using simulations done on the IEEE 39-bus test system.

The method is exclusively based on generator speed deviation which is straightforward and has a well-established accessibility at the generator shaft. The technique can be used directly as the main tool to predict generator coherency and for example system separation. It can also be used as a more extensive tool to provide control parameters for system stabilization equipment such as FACTS or PSS devices.

2. Rotor speed deviation as input parameter

Equation (1) shows the fundamental equation governing rotor dynamics. This equation is commonly referred to as the swing equation [20].

$$M\frac{d^2\delta}{dt^2} = P_m - P_e \qquad (1)$$

where M is the inertia coefficient, δ is the rotor angle, P_m is the mechanical power, and P_e is the electrical power.

Rotor angles have been extensively used for transient stability studies. Rotor angles as inputs need to be expressed relative to a common reference. This reference cannot be based on a single generator, since any instability in the reference generator makes the relative angles meaningless. In order to overcome this difficulty, the concept of system centre of inertia (COI) angle is used to derive a reference angle [21]. However, COI values in practice require continuous updates using real time measurements. This requires extra pre-processing and has significant errors. There is therefore the need for alternate inputs with simple implementation

The time derivative of rotor angle is the rotor speed deviation in electrical radians per second. Mathematically, it can be written as:

$$\frac{d\delta}{dt} = \Delta\omega = \omega - \omega_s \qquad (2)$$

where $\Delta\omega$ is the rotor speed deviation, ω is the rotor speed at a particular time, and ω_s is the synchronous speed.

It can also be shown that [22],

$$\frac{d\delta}{dt} = \left[\frac{\omega_0}{H}\int_{\delta_0}^{\delta} P_a d\delta\right]^{\frac{1}{2}} \qquad (3)$$

where H is the inertia constant and P_a is the difference between input mechanical power and output electromagnetic power. For stability to be attained after a disturbance, it is expected that $\frac{d\delta}{dt}$ will be zero in the first swing [23]. This condition gives rise to the equal area criterion which is a well-known classical transient stability criterion. From (2) and (3), it can also be written that

$$\Delta\omega = \left[\frac{\omega_0}{H}\int_{\delta_0}^{\delta} P_a d\delta\right]^{\frac{1}{2}} \qquad (4)$$

Equation (4) suggests speed deviation as a good input parameter for the prediction of transient stability status.

However, not many researchers have based their studies on rotor speed deviations. It is evidenced from (2) that the rate of change of rotor angle bears a direct relationship with the change in rotor speed. Thus rotor speed deviations also have the potential of giving information that can be extracted from rotor angles.

The maximum rotor speed deviation of a generator, in the first swing following a transient disturbance, will be much lower if it maintains synchronism with the other generators than if it goes out of step. Consequently, the maximum rotor speed deviation of each generator within the first swing can be used as an input parameter to predict the synchronism status of each generator of a power system following a transient disturbance. Mathematically,

$$x_i = Max\left(\Delta\omega_{ij}\right) \quad j = 1, 2, \ldots, m \qquad (5)$$

where x_i is the input data of algorithm to predict the synchronism status of generator i, $\Delta\omega_{ij}$ are the several rotor speed deviations of generator i sampled after the tripping of a line or bus, and m is the number of samples.

Very often, individual generators or groups of generators tend to oscillate together for a particular fault. Their rotor angle swings are dependent on each other and they evolve together with time [24]. This can be expressed by:

$$\delta_i(t) - \delta_j(t) \cong K_{ij}(t) \qquad 0 \le t \le t_{max} \qquad (6)$$

where i and j are pairs of generators, K_{ij} is a constant whose value may change with time.

The value of K_{ij} will be small and nearly constant within a coherent group. For a pair of generators which go

out of step, the value of K_{ij} will be large and may also largely vary with time. It follows from (6) that

$$\frac{d\delta_i(t)}{dt} - \frac{d\delta_j(t)}{dt} \cong K_{2ij}(t) \tag{7}$$

From which

$$\Delta\omega_i - \Delta\omega_j \cong K_{2ij}(t) \tag{8}$$

K_{2ij} is another constant whose value may also change with time.

Equation (8) shows that following a disturbance, the difference in speed deviation of coherent generators will be small and nearly constant while the difference in speed deviation of pairs or group of generators that go out of step will be large and also vary. Also, generators that remain stable after a disturbance, keep their coherency.

Rotor speed deviation of each generating unit can be obtained with the help of phasor measurement units (PMUs) [25, 26]. Thus algorithms based on rotor speed deviations can be implemented in the field.

3. Artificial neural networks as decision making tool

Artificial Neural Networks (ANNs) represent a modern and sophisticated approach to problem solving widely explored also for power system protection and control applications. ANNs perform actions similar to human reasoning, which relies upon experience gathered during a training process. Advantages of ANNs computing methodologies over conventional approaches include faster computation, learning ability, adaptive features, robustness and noise rejection [27].

ANNs are made up of a number of simple and highly interconnected processing elements, called neurons [28]. Figure 1 shows a mathematical model of an artificial neuron [29].

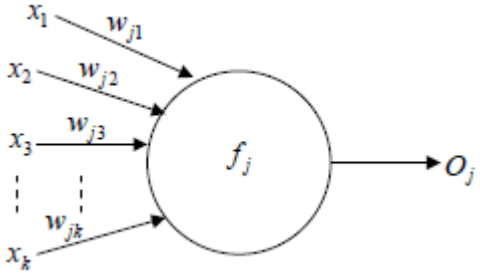

Fig. 1: Mathematical model of an artificial neuron

The mathematical model of a neuron as shown in fig. 1 is expressed as [28]:

$$O_j = f_j\left[\sum_k^N \left(w_{jk}\, x_k\right)\right] \tag{9}$$

where O_j is the output of a neuron, f_j is a transfer (activation) function which is differentiable and non-decreasing, w_{jk} is an adjustable weight that represents the connection strength, and x_k is the input of a neuron.

Various types of neural networks exist. These include multi-layer perceptrons, radial basis networks, Kohonen networks and recurrent networks [30]. Two commonly used neural networks are radial basis function (RBF) and multilayer perceptron (MLP) neural networks [30, 31]. The ANN used in this work is the Multi-Layer Perceptron neural network (MLPNN). MLPNN is a popular ANN with fast decision making capabilities [30-32].

4. Proposed prediction scheme for coherent generator groups

The proposed algorithm for the prediction of coherent generator groups makes use of the outputs of a scheme already developed in [33] that predicts the stability status of each generator after a disturbance. The scheme in [33] uses the maximum speed deviation of each generator, taken within the first cycle after the tripping of a line or bus, as input data. A trained multilayer perceptron neural network is used as a decision making tool to predict the stability status of each generator.

The coherency prediction scheme proposed in this paper uses the predicted stability status of each generator together with the following data, obtained in accordance with (5) and (8):

$$x_1 = Max(\Delta\omega_i) \tag{10}$$

$$x_2 = Max(\Delta\omega_j) \tag{11}$$

$$x_3 = \left|Max(\Delta\omega_i) - Max(\Delta\omega_j)\right| \tag{12}$$

where *i* is a reference generator in a coherent group and *j* is a generator to be placed in a coherent group. The reference generator is a generator with the highest $Max(\Delta\omega)$ value.

The coherent generator groups prediction scheme places all generators predicted to be transient stable, in one coherent group called 'S'. The scheme then focuses on only generators which are predicted to go out of step and determines whether they will belong to the same coherent group or different groups. Two multilayer perceptron neural networks namely MLPNN1 and MLPNN2 were trained for the prediction of coherent generator groups. Two MLPNNs were employed in order to increase the prediction accuracy of the proposed scheme. The prediction is done in three stages. MLPNN1 is responsible for the prediction of coherent groups in the first stage while MLPNN2 is responsible for the second and third stages. Both MLPNN1 and MLPNN 2 have the same architecture.

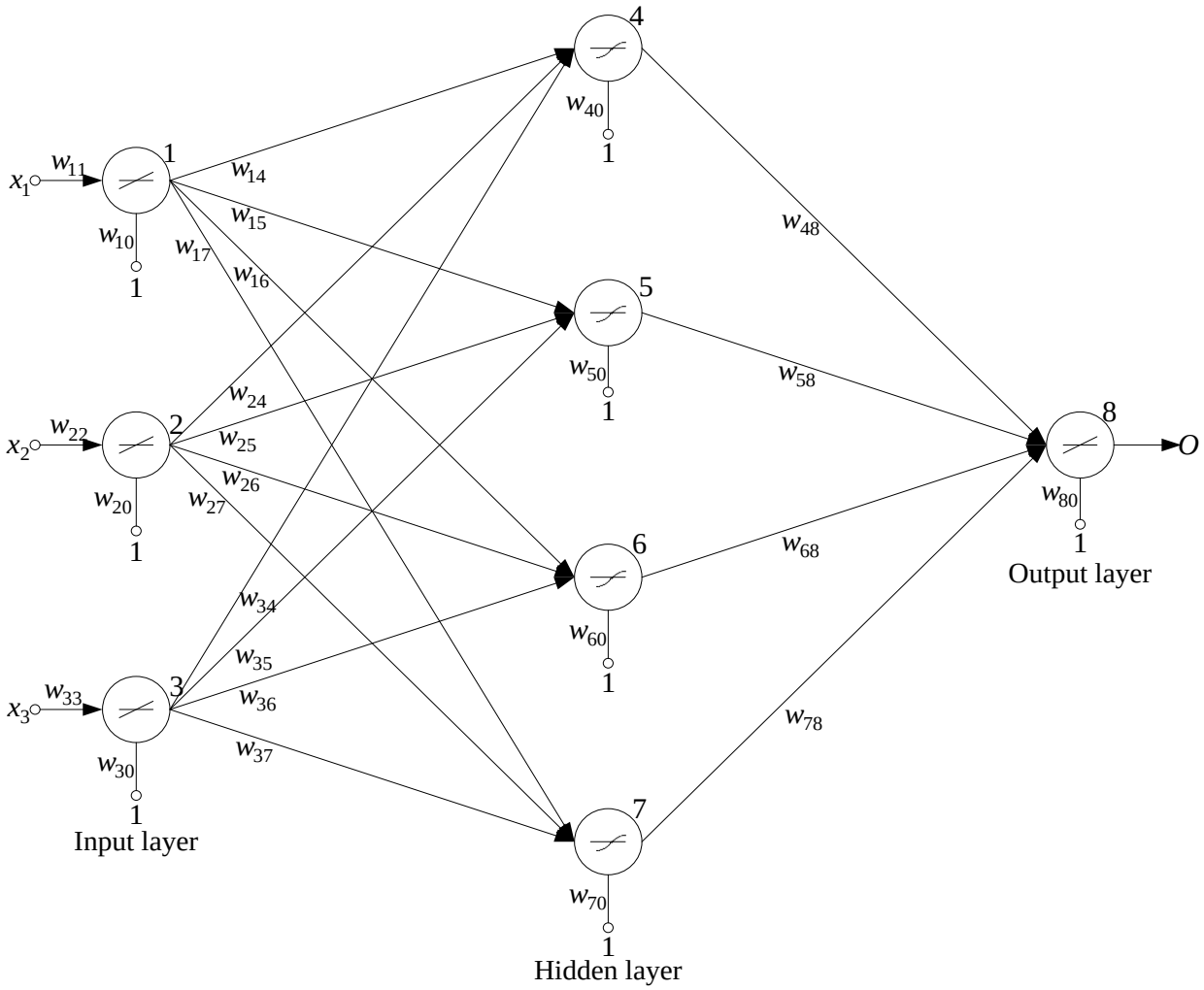

Fig. 2: Neural network architecture of coherency prediction scheme

The architecture of the neural networks is shown in fig. 2. In fig. 2, x_1 is the maximum speed deviation of the reference generator in a coherent group, x_2 is the maximum speed deviation of a generator which is to be placed in a coherent group, and x_3 is the absolute value of the difference between x_1 and x_2. *O* is the output of the neural network, which is expected to be either 1 or 0. An output of 1 means that the generators will be in different coherent groups, while an output of 0 means that the generators will be in the same coherent group.

Each MLPNN had 3 neurons in the input layer, 4 neurons in the hidden layer, and 1 neuron in the output layer. Each neuron had a bias. Biases have a constant input value of 1. The input and output neurons had 'purelin' transfer functions while the neurons in the hidden layer had 'tansig' transfer functions.

The output, O, of the MLPNN can be determined as follows:

The output, y_1 of neuron 1 is given by:

$$y_1 = f(x_1 w_{11} + w_{10}) = x_1 w_{11} + w_{10} \tag{13}$$

The output, y_2 of neuron 2 is given by:

$$y_2 = f(x_2 w_{22} + w_{20}) = x_2 w_{22} + w_{20} \tag{14}$$

The output, y_3 of neuron 3 is given by:

$$y_3 = f(x_3 w_{33} + w_{30}) = x_3 w_{33} + w_{30} \tag{15}$$

The output, y_4 of neuron 4 is given by:

$$y_4 = f(y_1 w_{14} + y_2 w_{24} + y_3 w_{34} + w_{40})$$

$$= \frac{e^{2(y_1 w_{14} + y_2 w_{24} + y_3 w_{34} + w_{40})} - 1}{e^{2(y_1 w_{14} + y_2 w_{24} + y_3 w_{34} + w_{40})} + 1} \tag{16}$$

The output, y_5 of neuron 5 is given by:

$$y_5 = f(y_1 w_{15} + y_2 w_{25} + y_3 w_{35} + w_{50})$$

$$= \frac{e^{2(y_1 w_{15} + y_2 w_{25} + y_3 w_{35} + w_{50})} - 1}{e^{2(y_1 w_{15} + y_2 w_{25} + y_3 w_{35} + w_{50})} + 1} \tag{17}$$

The output, y_6 of neuron 6 is given by:

$$y_6 = f(y_1 w_{16} + y_2 w_{26} + y_3 w_{36} + w_{60})$$

$$= \frac{e^{2(y_1 w_{16} + y_2 w_{26} + y_3 w_{36} + w_{60})} - 1}{e^{2(y_1 w_{16} + y_2 w_{26} + y_3 w_{36} + w_{60})} + 1} \quad (18)$$

The output, y_7 of neuron 7 is given by:

$$y_7 = f(y_1 w_{17} + y_2 w_{27} + y_3 w_{37} + w_{70})$$
$$= \frac{e^{2(y_1 w_{17} + y_2 w_{27} + y_3 w_{37} + w_{70})} - 1}{e^{2(y_1 w_{17} + y_2 w_{27} + y_3 w_{37} + w_{70})} + 1} \quad (19)$$

The output of the neural network, O which is the output of neuron 8 is given by:

$$O = f(y_4 w_{48} + y_5 w_{58} + y_6 w_{68} + y_7 w_{78} + w_{80})$$
$$= y_4 w_{48} + y_5 w_{58} + y_6 w_{68} + y_7 w_{78} + w_{80} \quad (20)$$

MLPNN1 and MLPNN2 were each trained using the Levenberg-Marquet training algorithm. The Levenberg– Marquardt algorithm which was independently developed by Kenneth Levenberg and Donald Marquardt, provides a numerical solution to the problem of minimizing a nonlinear function. It is fast, and has stable convergence. This algorithm is suitable for training small and medium-sized networks [34].

A flowchart of the proposed coherency prediction scheme is shown in fig. 3. The coherency prediction scheme is activated when a generator or system is predicted to be transient unstable following a disturbance. The scheme obtains the predicted stability status of each generator and sorts the generators into generators predicted to be stable and those predicted to be unstable. The generators predicted to be stable are all placed in a classified coherent group 'S', while the generators predicted to be unstable are placed in an unclassified coherent group 'U'. The scheme stops when only one generator is found in U. That generator is put in coherent group C_0. When more than one generator is found in U, the scheme sets a variable j to zero and obtains the maximum speed deviation (MSD) of each generator in U, in the 5th cycle after the tripping of a line or bus following a disturbance. j is a positive integer which indicates various coherent groups. The generator with the highest MSD value is placed in a classified coherent group 'Cj' and made the reference generator 'ref(jmod2+1)' in the group. The MSD of 'ref(jmod2+1)'is used as input x_1 of MLPNN(jmod2+1) for the placement of all other generators found in unclassified group U. For each of the other generators in U, its MSD is used as input x_2 of MLPNN(jmod2+1) for the placement of that generator in classified group 'Cj'. MLPNN(jmod2+1) determines whether a generator in U has to be added to group Cj or belongs to a different group. *j* is incremented when U still has a generator or generators. The scheme ends when no generator is found in U.

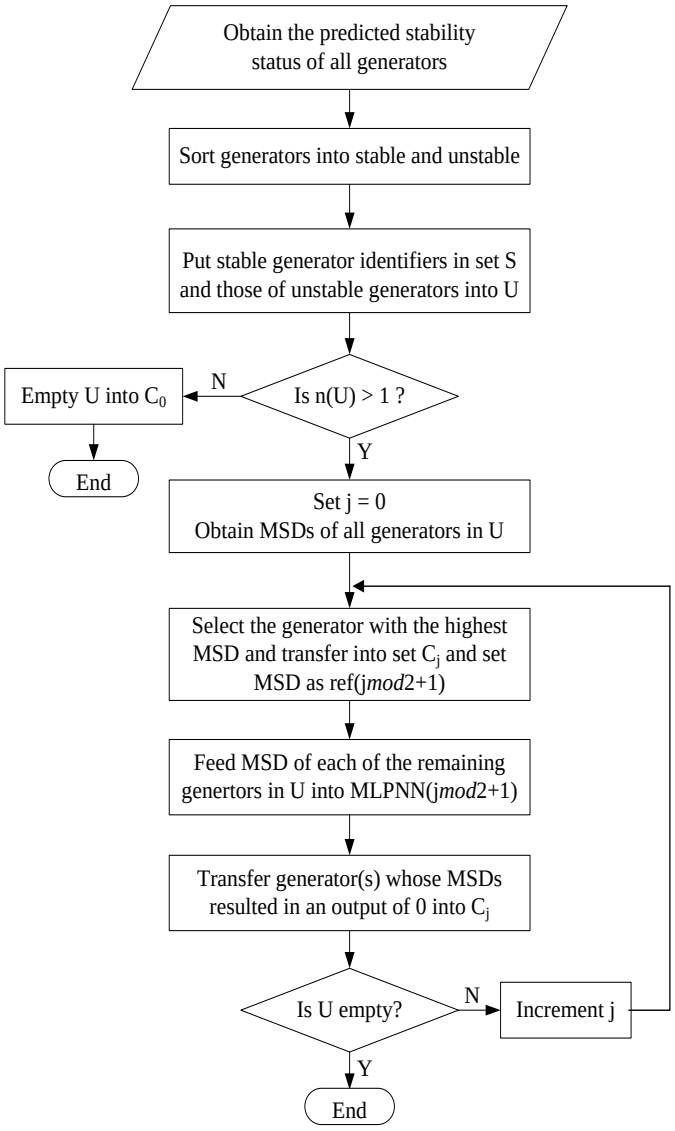

Fig. 3: Flowchart of proposed prediction scheme for coherency grouping

5. Configuration of test system

The coherent generator groups prediction scheme was test using the IEEE 39-bus test system, also known as the New England test system. The IEEE 39-bus test system is a standard test system that is widely used for

small and large signal stability studies [21,36–39]. This test system has also been used to test algorithms for online detection of coherent generator groups [11, 14, 15, 19] and the results compared with larger systems show that it is adequate for testing schemes such as the one that has been proposed in this paper. The test system is shown below as Fig. 4. It consists of 10 generators. Generator 1 (G1) is a generator representing a large system. Data for the modeling of the test system was obtained from [39].

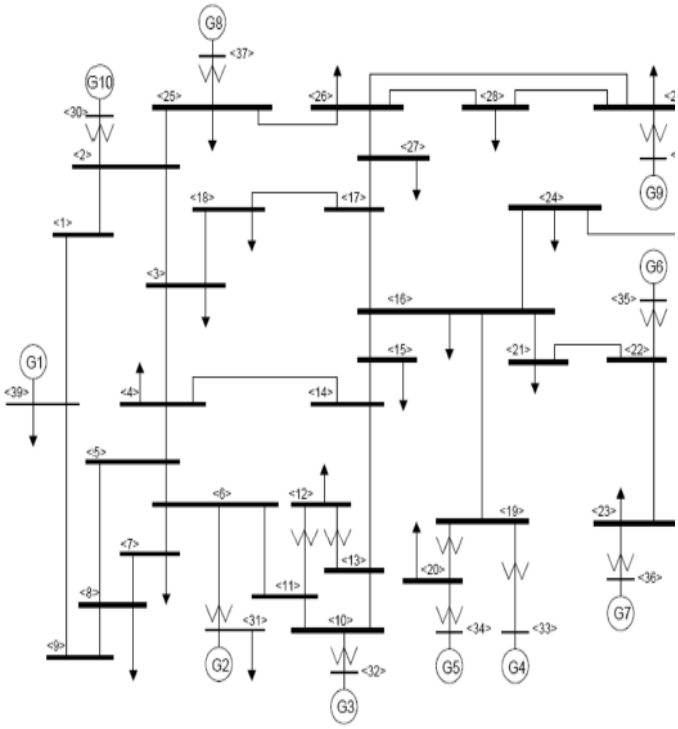

Fig. 4. IEEE 39-bus Test System

6. Simulations to generate training and test data

The modeling and simulation of the test system were carried out using the Power System Simulator for Engineers (PSSE) software [40]. Three-phase faults were created at various buses and on various lines. The system loading condition was also varied. The loading conditions used were: base load, base load increased by 5%, base load increased by 7%, and base load increased by 10%. The output data obtained from the simulations for testing the proposed scheme were rotor speed deviations of the generators. Rotor angles of the various generators were also obtained for the purpose of categorizing the simulation.

In each of the simulations, a generator is classified to be unstable or goes out of step when it accelerates or decelerates relative to the others such that the angular difference between it and the other generators is more than 180^o, 1 second after the tripping of a line or bus following a disturbance [36].

Coherent generator groups are formed whenever transient instability occurs. The generators in each group run in synchronism with each other but out of step with other generators in a different coherent group. Thus in the simulations, groups of generators whose angular difference did not exceed 180^o were deemed to be in one coherent group.

7. Training of multilayer perceptron neural networks

The two neural networks used in the proposed algorithm namely MLPNN1 and MLPNN2 were each trained using the Levenberg-Marquet training algorithm. The neural networks were trained using the MATLAB® software [41]. MLPNN1 was trained to give an output of '0' if the generator to be classified will be coherent with reference generator 'ref1'. Reference generator 'ref 1' is the generator with the highest MSD value in the second stage of the coherency prediction scheme. MLPNN1 gives an output of '1' if the generator to be classified will not be coherent with 'ref1'. MLPNN 2 was trained to give an output of '0' if the generator to be classified will be coherent with reference generator 'ref 2'. Reference generator 'ref 2' is the generator with the highest MSD value in the third stage. MLPNN 2 gives an output of '1' if the generator to be classified will not be coherent with 'ref 2'. MLPNN1 was trained using data from two transient unstable conditions. MLPNN2 was trained with data from one transient unstable condition. The input data for the training was obtained in accordance with (10) – (12).

Fig. 5 and fig. 6 show the training performance curves of MLPNN1 and MLPNN 2 respectively.

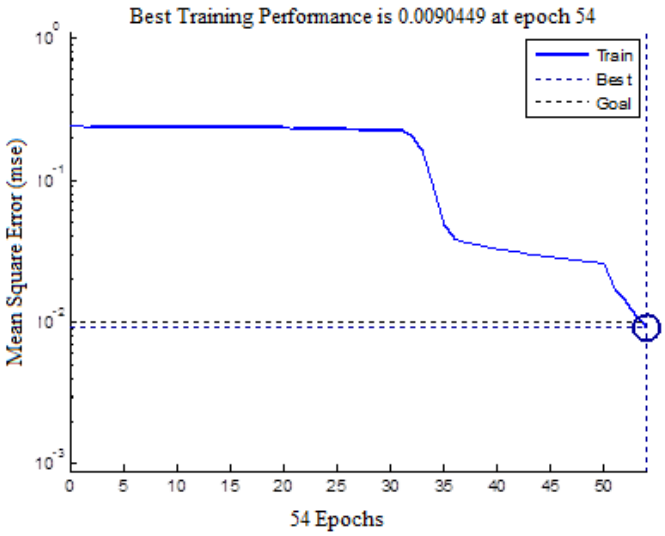

Fig. 5: Training performance of MLPNN1

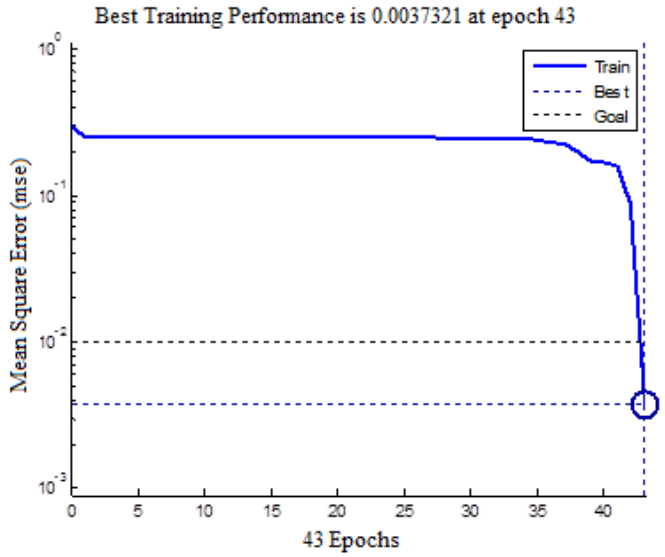

Fig. 6: Training performance of MLPNN 2

8. Test results

Data from 114 faults that led to transient instability and subsequent formation of coherent generator groups was used to test the proposed scheme. For example, fig. 7 shows a plot of rotor angles for a three-phase fault on the line between buses 5 and 8. The loading condition was at base load. The fault was applied at time $t_1 = 0.1s$ and lasted for 1 second. The line was tripped at time $t_2 = 1.1s$ resulting in some generators going out of step. Subsequently three coherent generator groups were formed. It can be observed from fig. 7 that generators 2 and 3 (G2 and G3) form one coherent group. Generators 4, 5, 6, 7, 8, 9, and 10 (G4, G5, G6, G7, G8, G9, and G10) form another coherent group. Generator 1 (G1) stands alone.

The corresponding plot of rotor speed deviations is shown in fig. 8. It can be seen from fig. 8 that the rotor speed deviations of the generators in each coherent group, immediately following the tripping of the line (at 1.1 seconds), are quiet close to each other. However, the speed deviations for different machines belonging to different coherent groups are clearly distinct. For example, whereas the speed deviations of generators 2 and 3 (G2 and G3) which form the first coherent group are much greater than 0.005, those in the second coherent group which comprises generators 4, 5, 6, 7, 8, 9 and 10 (G4, G5, G6, G7, G8, G9, and G10) are lower than 0.005. Also, the speed deviation of generator 1 (G1) which alone formed the third group is much lower than 0.001. Additionally, the difference between the speed deviations of generators in a coherent group is much lower than that between generators belonging to different coherent groups. Similar trends were observed for the other simulations that were carried out. Thus, the plots from the simulations corroborate what has been demonstrated theoretically that the speed deviations of the various generators in a system can be used to predict coherent generator groups following a disturbance.

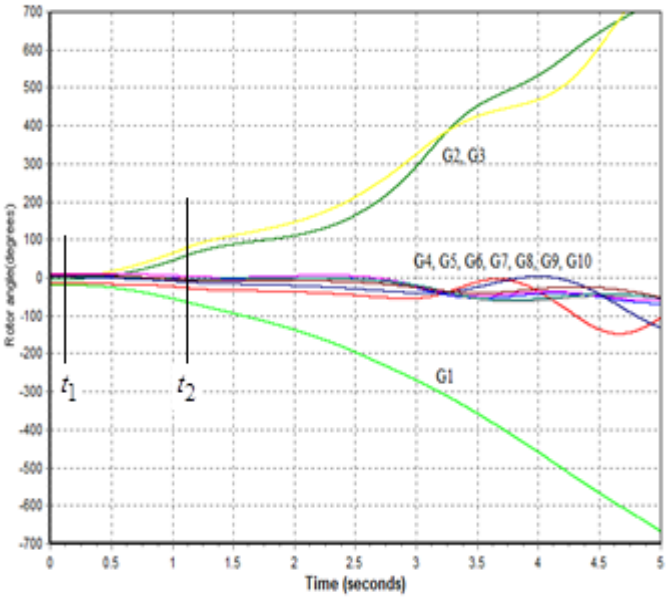

Fig. 7: Rotor angles for a three-phase fault on line between buses 5 and 8

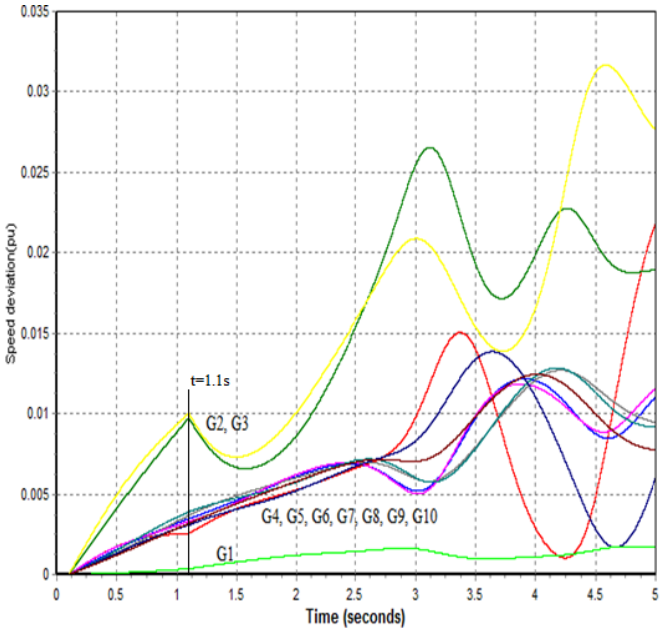

Fig. 8: Rotor speed deviations for a three-phase fault on line between buses 5 and 8

Table 1 shows the number of coherent groups that were formed in the 114 fault conditions simulated.

Table 1: Number of coherent groups formed for various fault conditions

No.	Number of fault conditions	Number coherent groups for each condition
1	83	2
2	31	3

For example, Table 2 shows the coherent groups formed for a three-phase fault on the line between buses 5 and 8. In the first stage of the proposed grouping algorithm, generators in group C were placed in coherent group S. The generators in groups A and B were placed in unclassified group U1. In the second stage of the algorithm, generator 3 which had the highest MSD (that is 0.0088) was made the reference generator, 'ref1'. Generator 3 was thus placed in classified coherent group C1. The scheme then determined whether or not generators 1 and 2 were in group C1. Generator 1 did not belong to group C1 so MLPNN1 was required to give an output of '1', which it did. Generator 2 belonged to group C1 and as expected, MLPNN1 gave an output of '0'. The algorithm ended at the second stage after placing generator 1 in group C2.

Table 2: Formed coherent groups for a fault on the line between buses 5 and 8

Group name	Generators
A	1
B	2 and 3
C	4, 5, 6, 7, 8, 9 and 10

Similar responses were obtained for the other 113 fault conditions. There were however, some grouping errors. The grouping error of the proposed scheme was found to be 8.78%.

9. Conclusion

This paper has presented an online scheme for predicting coherent generator groups that may be formed following transient instability. The proposed scheme uses rotor speed deviations obtained in the 5^{th} cycle after the tripping of a line or bus following a disturbance. The use of rotor speed deviation which can be measured in the field with the help of phasor measurement units makes the implementation of the scheme feasible. The use of only one input parameter as well as a simple input data processing approach also makes the scheme simple to implement.

References

1. Power Systems Transient Stability – A Grand Computing Challenge. NPAC Technical Report – SCCS 549, August 1992.
2. *Power Swing and OOS Considerations on Transmission Lines*, A report to the Power System Relaying Committee of the IEEE Power Engineering Society, 2005.
3. You H., Vittal V., and Yang Z.: *Self-Healing in Power Systems: An Approach using Islanding and Rate of Frequency Decline-Based Load Shedding*. In: IEEE Trans. on Power Systems, vol.18, no.1, Feb. 2003, p. 174-181.
4. El-Werfelli M., Brooks J. and Dunn R.: *Controlled islanding scheme for power systems*. 43rd Universities Power Conference, Padova, Sept. 2008.
5. You H., Vittal V. and Wang X.: *Slow Coherency-Based Islanding*. In: IEEE Trans. on Power Systems, vol. 19, no. 1, Feb. 2004, p. 483-491.

6. Yang B., Vittal V. and Heydt G. T.: *Slow Coherency Based Controlled Islanding – A Demonstration of the Approach on the August 14, 2003*. In: IEEE Trans. Power Syst., vol. 21, no. 4, Nov. 2006, p. 1840–1847.
7. Tortos J. Q. and Terzija V.: *Controlled islanding strategy considering power system restoration constraints*. In: Power and Energy Society general meeting, San Diego, Jul. 2012.
   Diao R., Vittal V., Sun K., Kolluri S., Mandal S. and Galvan F.: *Decision tree assisted controlled islanding for preventing cascading events*. In: IEEE/PES Power Systems Conference and Exposition, Seattle, Mar. 2009.
8. Smith G. and Sun K.: *A Controlled System Separation Scheme and Related Dynamic Studies for New York State Transmission System Using Synchrophasors*. In: Electric Power Research Institute, New York, Proposal for DOE FOA-0000036, Jun. 2009.
9. Tang K. and Venayagamoorthy, G. K.: *Online coherency analysis of synchronous generators in a power system*. In: Proc. IEEE PES Innovative Smart Grid Technologies Conference (ISGT), Washington DC, 2014, pp. 1-5.
10. Wang X., Vittal V. and Heydt G. T.: *Tracing generator coherency indices using the continuation method: A novel approach*. In: IEEE Transactions on Power Systems, vol. 20, no. 3, Aug. 2005, p. 1510-1518.
11. Senroy N.: *Generator Coherency Using the Hilbert–Huang Transform*. In: IEEE Transactions on power systems, vol. 23, no. 4, Jun. 2008, p. 1701-1708.
12. Jonsson M., Begovic M. and Daalder J.: *A New Method Suitable for Real-Time Generator Coherency Determination*. In: IEEE Transactions on Power Systems, vol. 19, no. 3, Aug. 2004, p. 1473-1482.
13. Aghamohammadi M. R. and Tabandeh S. M.: *Online Coherency Identification Based on Correlation Characteristics of Generator Rotor Angles*. In: Proc. IEEE International Conference on Power and Energy (PECon), Kota Kinabalu, 2012, p. 499-504.
14. Yang S., Zhang B., Su F. and Bo Z.: *A Real-time Identification Scheme of Coherent Generators based on the WAMS information*. In: Proc. International Conference on Power System Technology (POWERCON 2014), Chengdu, 2014, p. 388-394.
15. Feng K., Zhang Y., Liu Z., Li T. and Ma H.: *A Wide Area Information Based Online Recognition of Coherent Generators in Power System*. In: Power System Technology, vol. 38, no. 8, 2014, p. 2082-2086.
16. Wei J., Kundur D. and Butler-Purry K. L.: *A Novel Bio-Inspired Technique for Rapid Real-Time Generator Coherency Identification*. In: IEEE Transactions on Smart Grid, vol. 6, no. 1, Aug. 2014, p. 178-188.
17. Susuki Y., and Mezic´ I.: *Nonlinear Koopman Modes and Coherency Identification of Coupled Swing Dynamics*. In: IEEE Transactions on Power Systems, vol. 26, no. 4, Feb. 2011, p. 1894-1904.
18. Susuki Y. and Mezic´ I. *Correction to "Nonlinear Koopman Modes and Coherency Identification of Coupled Swing Dynamics*. In: IEEE Transactions on Power Systems, vol. 26, no. 4, Sept. 2011, p. 2584.
19. Nagrath I. J. and Kothari D. P.: Power System Stability. In: *Power System Engineering*: Tata Mcgraw-Hill Publishing Compay Limited, New Delhi, pp. 484-491.
20. Rajapakse A. D., Gomez F., Nanayakkara O. M. K. K., Crossley P. A. and Terzija V. V.: *Rotor angle stability prediction using post-disturbance voltage trajectory patterns*. In: IEEE Transactions on Power Systems, vol. 25, no. 2, May 2010, p. 945-956.
21. Kundur P.: Synchronous Machines Theory and Modelling. In: *Power System Stability and Control*: McGraw-Hill, Inc., USA, 1994, pp. 128-131.
22. Sadat H.: *Stability*. In: Power Systems Analysis: Tata McGraw-Hill Publishing Company Limited, New Delhi, 2002, pp. 460-464.
23. Rudnick H., Patino R. I. and Brameller A.: *Power-System Dynamic Equivalents: Coherency Recognition via the Rate of Change of Kinetic Energy*. In: IEE Proceedings on Gen. Trans. and Dist., vol. 128, no. 6, Nov. 1981, p. 325-333.
24. Abdelaziz Y. A., Ibrahim A. M. and Hasan Z. G.: *Phasor Measurement Units for Out of Step Detection*. In: Proc. 8th International Conference on Electrical Engineering (ICEENG 2012), Cairo, Egypt, May 2012, p. 1-21.
25. Satyanarayana K., Prasad B. K. V. and Rajesh G.: *Transient stability enhancement of power system*

using intelligent technique. In: International Journal of Advanced Engineering Research and Studies, vol. 1, no. 1, Oct. 2011, p. 10-14.
26. Rebizant W.: *ANN based detection of OS conditions in power system*. In: Proc. 12th International conference on Power System Protection, Bled, Solvania, 2000, p. 51-56.
27. Frimpong E. A. and Okyere P. Y.: *Forecasting the Daily Peak Load of Ghana Using Radial Basis Function Neural Network and Wavelet Transform*. In: Journal of Electrical Engineering, Mar. 2010, vol. 10, no. 1, pp. 15-18.
28. Momeni A., Maleki S. and Khajeh K.: *Analysts' Equity Forecasts Using of Multi-layer Perception (MLP)*. In: Advances in Environmental Biology, vol. 8, no. 1, Jan. 2014, p. 207-21.
29. McGarry K. J., Wermter S. and MacIntyre J.: *Knowledge Extraction from Radial Basis Function Networks and Multi-layer Perceptrons*. In: Proc. International Joint Conference on Neural Networks, Washington D.C., 1999, p. 1-4.
30. Kavousifard A. and Samet H.: *Consideration effect of uncertainty in power system reliability indices using radial basis function network and fuzzy logic theory*. In: Neurocomputing, vol. 74, no. 17, Oct. 2011, p. 3420-3427.
31. Angel A. D., Glavic M. and Wehenkel L.: *Using Artificial Neural Networks to Estimate Rotor Angles and Speeds from Phasor Measurements*. In: Neurocomputing, vol. 70, no. 16-18, Oct. 2007, p. 2668-2678.
32. Yu H. and Wilamowski, B. M.: *Intelligent Systems*. In: Industrial Electronics Handbook, 2nd Edition, CRC press, 2011, p. 12-1 to 12-15.
33. Frimpong E. A., Asumadu J. and Okyere P. Y.: Neural Network and Speed Deviation Based Generator Out-Of-Step Prediction Scheme. In: *Journal of Electrical and Electronic Engineering*, vol. 15, no. 2, Jul. 2015, p. 1-8.
34. Stanton S. E., Slivinsky C., Martin K. and Nordstorm J.: *Application of phasor measurement and partial energy analysis in stabilizing large disturbances*. In: IEEE Transaction on Power Systems, vol. 10, no. 1, Feb. 1995, p. 297-306.
35. Amjady N.: *Application of a new fuzzy neural network to transient stability prediction*. In: Proc. IEEE Power Engineering Society General Meeting, San-Francisco, Jun. 12-16, 2005, p. 636-643.
36. Amjady N. and Majedi S. F.: *Transient stability prediction by a hybrid intelligent system*. In: IEEE Transactions on Power Systems, vol. 22, no. 3, Aug. 2007, p. 1275-1283.
37. Liu C. W., Su M. C., Tsay S. S. and Wang Y. J.: *Application of a novel fuzzy neural network to real-time transient stability swings prediction based on synchronized phasor measurements*. In: IEEE Trans. Power App. Syst., vol 14, no. 2, May 1999, p. 685-692.
38. Rovnyak S., Kretsinger S., Thorp J. and Brown D.: *Decision trees for real-time transient stability prediction*. In: IEEE Transactions on Power Systems, vol. 9, no. 3, Aug. 2002, p. 1417-1426.
39. Song Y.: *Design of Secondary Voltage and Stability Controls with Multiple Control Objectives*. In: PhD dissertation, School of Electrical and Computer Engineering, Georgia Institute of Technology, Georgia, USA, 2009.
40. Power System Simulator for Engineers, PSS®E University Edition, 2013
41. MATLAB® R2013a, MathWorks Company, 2013.